O-Atom Transfer in Fe Complexes

Thermally Induced Stoichiometric and Catalytic O-Atom Transfer by a Non-Heme Iron(III)–Nitro Complex: First Example of Reversible $\{Fe–NO\}^7 \leftrightarrow Fe^{III}\text{-}NO_2$ Transformation in the Presence of Dioxygen**

*Apurba K. Patra, Raman K. Afshar, John M. Rowland, Marilyn M. Olmstead, and Pradip K. Mascharak**

In recent years, a few Fe[1] and Co[2] porphyrin complexes with a bound nitro group have been employed to transfer an oxygen atom to substrates such as PPh_3, Me_2S, and styrene.

[*] Prof. Dr. P. K. Mascharak, Dr. A. K. Patra, R. K. Afshar, Dr. J. M. Rowland
Department of Chemistry and Biochemistry
University of California
Santa Cruz, CA 95064 (USA)
Fax: (+1) 831-459-2935
E-mail: pradip@chemistry.ucsc.edu
Dr. M. M. Olmstead
Department of Chemistry
University of California
Davis, CA 95616 (USA)

[**] Financial support from NIH (GM 61636) is gratefully acknowledged. The Bruker SMART 1000 diffractometer was funded in part by an NSF Instrumentation Grant CHE-9808259.

 DOI: 10.1002/ange.200352070

Other transition-metal nitro complexes[3] have also been successfully used in stoichiometric and catalytic O-atom transfer to CS_2, CO, alcohols, and alkenes. However, no non-heme iron complex with a bound nitrite group has been shown to perform O-atom transfer to any such substrate. In this paper we report the first non-heme Fe^{III} complex $[(PaPy_3)Fe(NO_2)](ClO_4)$ (**1**) derived from the *N*,*N*-bis-(2-pyridylmethyl)amine-*N*-ethyl-2-pyridine-2-carboxamide ligand ($PaPy_3H$ = *N*-[*N*,*N*-bis(2-pyridylmethyl)aminoethyl]-2-pyridinecarboxamide; H is the dissociable amide proton), which promotes stoichiometric and catalytic O-atom transfer to PPh_3 under mild conditions. We also report that the {Fe–NO}^{7}-type species $[(PaPy_3)Fe(NO)](ClO_4)$ (**2**) is the intermediate in the nitrite-to-nitrosyl conversion following O transfer to PPh_3. Since **2** is rapidly converted into **1** via electrophilic attack of dioxygen to the coordinated NO in **2**, the O-atom transfer reaction can be made catalytic in an atmosphere of dioxygen. We also report that in absence of dioxygen, the {Fe–NO}^{7} intermediate **2** is converted into the μ-oxo diiron(III) species $[(PaPy_3)FeOFe(PaPy_3)](ClO_4)_2$ (**3**) via a disproportionation reaction, as reported by Lippard and co-workers.[4] Complex **3** is the final product obtained from the O-atom transfer reaction.

Complex **1** has been synthesized by the addition of $[Fe(dmf)_6](ClO_4)_3$ to a mixture of $PaPy_3H$ and NEt_3 (1:1) in MeCN following the addition of $NaNO_2$. Coordination of the deprotonated carboxamido nitrogen atom to the Fe^{III} center is indicated by a red shift in the position of ν_{CO} (1634 compared to 1666 cm^{-1} for the free ligand). Complex **1** displays a rhombic EPR spectrum with *g* values at 2.347, 2.212, and 1.902. This large anisotropy is typical of the $(t_{2g})^5$ configuration for low-spin Fe^{III} ($S = 1/2$) centers, due to strong the spin–orbit interaction of the "hole" in the t_{2g} subshell.[5] The structure of the cation of **1** is shown in Figure 1;[6] the Fe^{III} center is in a distorted octahedral geometry. Three pyridine N atoms and the *tert*-amine N atom comprise the equatorial plane while the carboxamido N atom occupies one of the axial positions. The N-bound NO_2^- ligand is positioned *trans* to the carboxamido N atom; the length of the $Fe{-}N_{(amide)}$ bond is 1.8563(13) Å. This value is very close to the $Fe{-}N_{(amide)}$ distances noted in the $[(PaPy_3)Fe(X)]^+$ ($X = Cl^-$, CN^-) species.[7] The oxygen atoms of the nitro group are disordered and were refined with 0.752(5) occupancy for one set (O2A and O3A) and 0.248(5) occupancy for the other set (O2B and O3B) of oxygen atoms. The average Fe-N-O angles are 116.31(6)° and 120.90(6)°, while the average $Fe{-}N_{(py)}$ and $Fe{-}N_{(amine)}$ bond lengths are 1.9713(14) and 1.9847(14) Å, respectively.

The {Fe–NO}^{7} intermediate, complex **2**, has been independently synthesized by reacting one equivalent of NO(g) with a mixture of $PaPy_3H$, NEt_3, and $[Fe(MeCN)_4](ClO_4)_2$ (1:1:1) in thoroughly degassed MeCN. The IR spectrum of the dark brown-red solid displays ν_{NO} at ~1613 cm^{-1}, a value comparable to other {Fe–NO}^{7}-type complexes. The X-band EPR spectrum displays a strong signal at $g \approx 2.002$ indicating an $S = 1/2$ electronic ground state. The structure of $[(PaPy_3)Fe(NO)]^+$, the cation of complex **2**, is shown in Figure 2.[8] The distorted octahedral geometry around the iron center in this {Fe-NO}^{7} nitrosyl is similar to that observed in **1**. The Fe–N(O) bond length is 1.7515(16) Å and the Fe-N-O angle is 141.29(15)°. Both the Fe–N(O) distance and the smaller Fe-N-O angle of **2** are typical of the {Fe–NO}^{7} iron nitrosyl complexes.[9] The N–O bond length in **2** (1.190(2) Å) is close to that of free NO (1.15 Å) but far from that found in NO^- (1.26 Å).

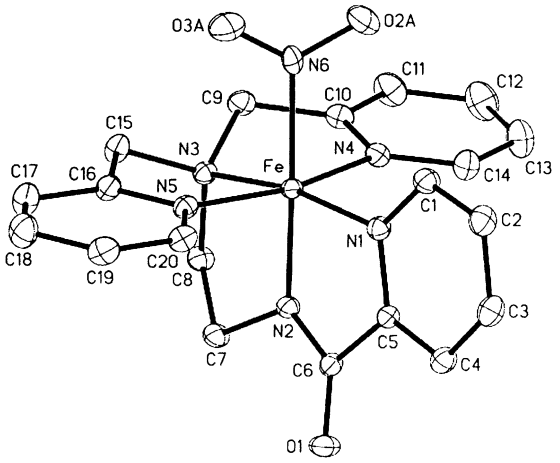

Figure 1. ORTEP diagram of $[(PaPy_3)Fe(NO_2)]^+$, the cation of **1**, showing the atom labeling scheme. All H atoms and the MeCN molecules present as solvent of crystallization have been omitted for clarity. Selected bond lengths [Å] and bond angles [°]: Fe-N1 1.9856(14), Fe-N2 1.8563(13), Fe-N3 1.9847(14), Fe-N4 1.9648(15), Fe-N5 1.9637(14), Fe-N6 2.0436(15), N6-O2(av) 1.240(5), N6-O3(av) 1.182(5); Fe-N6-O2(av) 116.31(6), Fe-N6-O3(av) 120.90(6), N6-Fe-N2 175.18(6), N1-Fe-N2 83.05(6), N1-Fe-N3 168.77(6), N1-Fe-N4 97.15(6), N1-Fe-N5 96.31(6), N2-Fe-N3 85.78(6), N2-Fe-N4 96.21(6), N2-Fe-N5 88.13(6), N3-Fe-N4 82.80(6), N3-Fe-N5 84.53(6), N3-Fe-N6 96.68(6), N4-Fe-N5 166.26(6), N4-Fe-N6 88.23(6), N5-Fe-N6 87.98(6).

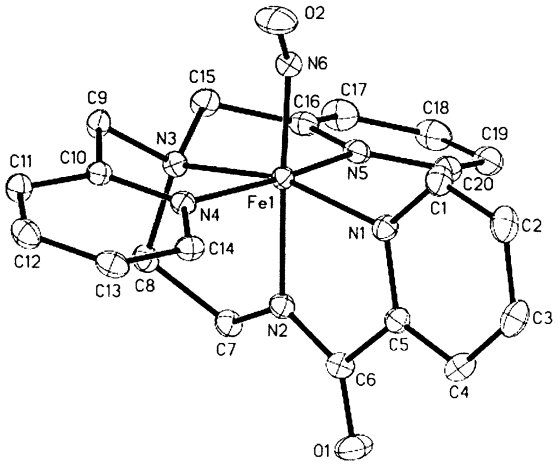

Figure 2. ORTEP diagram of $[(PaPy_3)Fe(NO)]^+$, the cation of **2**, showing the atom labeling scheme. All H atoms and the MeCN molecules present as solvent of crystallization have been omitted for clarity. Selected bond lengths [Å] and bond angles [°]: Fe-N1 1.9801(15), Fe-N2 1.9577(15), Fe-N3 1.9946(16), Fe-N4 1.9836(15), Fe-N5 1.9990(15), Fe-N6 1.7515(16), N6-O2 1.190(2); Fe-N6-O2 141.29(15), N6-Fe-N2 176.91(7), N1-Fe-N2 80.07(6), N1-Fe-N3 164.15(6), N1-Fe-N4 95.44(6), N1-Fe-N5 98.14(6), N2-Fe-N3 84.29(6), N2-Fe-N4 91.38(6), N2-Fe-N5 86.08(6), N3-Fe-N4 82.33(6), N3-Fe-N5 83.25(6), N3-Fe-N6 98.80(7), N4-Fe-N5 165.53(6), N4-Fe-N6 88.92(7), N5-Fe-N6 94.38(7).

Complex **3**, the end product of the catalytic cycle, has been independently synthesized by allowing a stoichiometric amount of dioxygen to react with a mixture of $PaPy_3H$, NEt_3, and $[Fe(MeCN)_4](ClO_4)_2$ (1:1:1) in MeCN. The IR spectrum of **3** shows a strong band at 785 cm^{-1}, which corresponds to $\tilde{\nu}_{Fe\text{-}O\text{-}Fe}$. The structure of $[(PaPy_3)FeOFe(PaPy_3)]^{2+}$, the cation of **3**, is shown in Figure 3.[10] The high-spin ($S = 5/2$) nature of

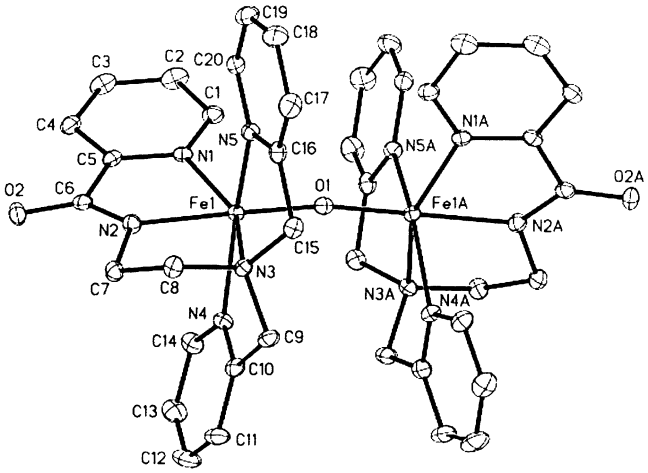

Figure 3. ORTEP diagram of $[(PaPy_3)FeOFe(PaPy_3)]^{2+}$, the cation of **3**, showing the atom labeling scheme. All H atoms and the EtOH molecules present as solvent of crystallization have been omitted for clarity. Selected bond lengths [Å] and bond angles [°]: Fe1-N1 2.144(3), Fe1-N2 2.064(4), Fe1-N3 2.200(3), Fe1-N4 2.181(3), Fe1-N5 2.169(3), Fe1-O1 1.8039(7); Fe1-O1-Fe1A 170.7(2), O1-Fe1-N2 172.19(10), N1-Fe1-N2 75.54(13), N1-Fe1-N3 154.04(13), N1-Fe1-N4 106.22(13), N1-Fe1-N5 98.54(13), N1-Fe1-O1 99.01(12), N2-Fe1-N3 79.51(13), N2-Fe1-N4 81.55(14), N2-Fe1-N5 92.53(14), N3-Fe1-N4 76.72(13), N3-Fe1-N5 75.37(13), N3-Fe1-O1 106.50(12), N4-Fe1-N5 152.07(13), N4-Fe1-O1 94.84(15), N5-Fe1-O1 93.83(13).

the two Fe^{III} centers in **3** is indicated by the longer Fe–N bond lengths compared to the structurally characterized low-spin Fe^{III} complexes of $PaPy_3H$ ligand. The average $Fe–N_{(py)}$ and $Fe–N_{(amine)}$ bond lengths are 2.164(3) and 2.200(3) Å, respectively, while the $Fe–N_{(amide)}$ bond is 2.064(4) Å. These bond lengths are similar to other μ-oxo diiron(III) complexes with high-spin Fe^{III} centers.[11] To the best of our knowledge, **3** is the first structurally characterized μ-oxo diiron(III) complex with amido nitrogen-atom coordination.

When a burgundy red solution of **1** in MeCN (λ_{max} = 510 nm) is warmed with PPh_3 at 45 °C under 1 atm of dioxygen, Ph_3PO is rapidly formed in the reaction mixture. Formation of Ph_3PO can be monitored by either ^{31}P NMR spectroscopy or by HPLC. The rates of O-atom transfer (K_{obs}) have been measured in MeCN in the presence of 100 equiv of PPh_3 under 1 atm of dioxygen. The psuedo-first-order rate constants are 1.12×10^{-4} and 2.65×10^{-4} s^{-1} at 45 °C and 65 °C, respectively. However, at temperatures above 65 °C, significant decomposition of **2** (leading to the formation of **3**) is observed. When **1** is heated with PPh_3 in MeCN without any added oxygen, the O-atom transfer reaction proceeds according to the equation $[(PaPy_3)Fe(NO_2)]^+ + PPh_3 \rightarrow [(PaPy_3)Fe(NO)]^+ + Ph_3PO$, and one obtains just one equivalent of Ph_3PO irrespective of the amount of PPh_3 in the reaction mixture. Under such strictly anaerobic conditions, the intermediate {Fe-NO}^{7} species **2** can be identified in the reaction mixture by UV/Vis spectroscopy by a strong band at ≈475 nm.

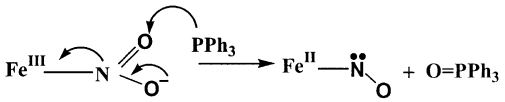

O-atom transfer from **1** results in an effective reduction of the metal center and generation of the {Fe–NO}^{7} species **2**. If heating is continued in absence of dioxygen, **2** eventually decomposes to the μ-oxo diiron(III) complex **3** (λ_{max} = 430 nm) presumably via a transient $\{FeNO\}_2$ species with an N–N bond, as suggested by Lippard and co-workers.[4] The **2**→**3** transformation can also be monitored by UV/Vis spectroscopy. One can isolate pure **3** from the reaction mixture after single turnover. This confirms that **3** does not promote O-atom transfer.

In MeCN, **2** reacts rapidly with dioxygen to form **1**. This nitrosyl-to-nitrite conversion in a non-heme system is unique[12] and can be easily monitored by UV/Vis spectroscopy. The reaction allows the O-atom transfer reaction to be catalytic under an atmosphere of pure dioxygen and in the presence of excess PPh_3. At 45 °C, the turnover number (TN)[13] is 37 after 1 h while at 65 °C, the TN increases to 84.[14] The overall catalytic efficiency of **1** becomes somewhat curtailed by the fact that during the **2**→**1** conversion, a small portion (< 1 %) of **2** is converted to **3** (as evidenced by UV/Vis spectroscopy) and thus the effective concentration of **1** in the reaction mixture decreases over time. Such damage can be minimized (easily monitored by the observation of the burgundy-red color of the solution) by running the O-atom transfer reaction at lower temperatures. The catalytic process can be schematically described as follows:

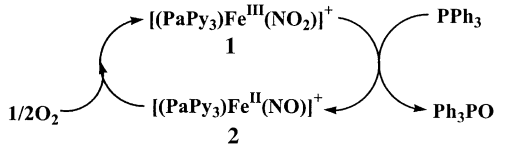

In summary, $[(PaPy_3)Fe(NO_2)](ClO_4)$ (**1**) is the first example of a non-heme iron–nitro species that promotes stoichiometric and catalytic O-atom transfer to PPh_3. We have also isolated and identified the intermediate $[(PaPy_3)Fe(NO)](ClO_4)$ (**2**), a {Fe–NO}^{7} species. This reversible nitrite-to-nitrosyl conversion is also the first example in non-heme iron chemistry. Formation of the μ-oxo diiron(III) complex $[(PaPy_3)FeOFe(PaPy_3)](ClO_4)_2$ (**3**) is the termination product of the catalytic cycle.

Experimental Section

1: A solution of $PaPy_3H$ (0.20 g, 0.58 mmol) in MeCN (15 mL) was added to a solution of $[Fe(DMF)_6](ClO_4)_3$ (0.46 g, 0.58 mmol) in MeCN (10 mL). Then a solution of NEt_3 (0.06 g, 0.58 mmol) in MeCN

(7 mL) was slowly added with constant stirring. The deep-violet solution was stirred for 30 min and then solid $NaNO_2$ (0.125 g, 1.81 mmol) was added. The color of the reaction mixture changed slowly to red after 3 h, which was then filtered to remove excess $NaNO_2$ and concentrated to 15 mL. Et_2O (15 mL) was then added and the solution was stored at −20 °C for 24 h. The dark-red blocks were filtered and washed with Et_2O (0.32 g, 88 % yield). Crystals of $[(PaPy_3)Fe(NO_2)](ClO_4)\cdot 2\,MeCN$ (**4**·2 MeCN) were grown via diffusion of Et_2O into solution of the complex in MeCN at 4 °C. Elemental analysis calcd (%) for $C_{24}H_{26}ClFeN_8O_7$ (**4**·2 MeCN): C 45.77, H 4.13, N 17.78; found: C 45.71, H 4.09, N 17.71. FTIR (KBr): $\tilde{\nu} = 3065$ (w), 2958(w), 2852 (w), 2249 (m), 1636 (vs), 1607 (vs), 1470 (m), 1446 (m), 1364 (s), 1280 (m), 1090 (vs), 764 (m), 622 cm^{-1} (m). Electronic absorption spectrum in MeCN, λ_{max} (in nm) (ε in $M^{-1}cm^{-1}$): 512 (2730), 390 (sh, 2190), 360 (sh, 3900), 340 (sh, 4120).

2: A solution of $PaPy_3H$ (0.122 g, 0.35 mmol) and NEt_3 (0.05 g, 0.49 mmol) in MeCN (20 mL) was thoroughly degassed by freeze-pump-thaw cycles. Solid $[Fe(MeCN)_4](ClO_4)_2$ (0.148 g, 0.35 mmol) was added to the frozen MeCN solution, which was then allowed to warm to room temperature. The dark brown-red solution obtained was stirred for 30 min at room temperature and then cooled to 0 °C, where NO (11 mL, 0.49 mmol) was introduced to the reaction flask via a gas-tight syringe following evacuation. The resulting deep-brown reaction mixture was then stirred for 1 h. Et_2O (25 mL) was then added, and the reaction mixture was stored at −20 °C for 12 h. Dark brown-red blocks were filtered and washed with small portions of Et_2O and dried (0.135 g, 62 % yield). Elemental analysis calcd (%) for $C_{24}H_{26}ClFeN_8O_6$ (**2**·2 MeCN): C 46.96, H 4.23, N 18.25; found: C 46.86, H 4.19, N 18.24. FTIR (KBr): $\tilde{\nu} = 3072$ (w), 2942(w), 2860 (w), 2284 (w), 2249 (m), 1613 (vs), 1590 (vs), 1454 (m), 1401 (w), 1373 (w), 1284 (m), 1219 (w), 1085 (vs), 761 (m), 620 cm^{-1} (m). Electronic absorption spectrum in MeCN, λ_{max} (in nm) (ε in $M^{-1}cm^{-1}$): 830 (50), 476 (4300), 390 (sh, 3130), 370 (3170).

3: A solution of $PaPy_3H$ (0.1 g, 0.29 mmol) and NEt_3 (0.035 g, 0.35 mmol) in MeCN (10 mL) was thoroughly degassed using freeze-pump-thaw cycles. Solid $[Fe(MeCN)_4](ClO_4)_2$ (0.122 g, 0.29 mmol) was added to the frozen MeCN solution, which was then allowed to warm to room temperature. The dark brown-red solution obtained was stirred for 1 h and then pure dioxygen (6.5 mL measured with the aid of a gas-tight syringe) was added. Upon further stirring, the color of the reaction mixture changed to red-orange. Dry Et_2O (17 mL) was then added, and the mixture was stored at −20 °C for 12 h. Red-orange microcrystals of **3** were obtained by filtration and washed with Et_2O and dried (0.125 g, 85 % yield). Single crystals of $[(PaPy_3)FeO\text{-}Fe(PaPy_3)](ClO_4)_2\cdot 3\,EtOH$ (**3**·3 EtOH) suitable for diffraction studies were grown from a 1:1 (v/v) MeOH/EtOH solution by slow evaporation. Elemental analysis calcd (%) for $C_{46}H_{58}Cl_2Fe_2N_{10}O_{14}$ (**3**·3 EtOH): C 47.73, H 5.05, N 12.10; found: C 47.66, H 5.01, N 12.12. FTIR (KBr): $\tilde{\nu} = 3585$ (m), 3079(w), 2928(w), 2870 (w), 1622 (vs), 1594 (vs), 1567(s), 1486 (w), 1445 (m), 1399 (m), 1294 (m), 1094 (vs), 880(w), 784(vs), 624 cm^{-1} (m). Electronic absorption spectrum in MeCN, λ_{max} (in nm) (ε in $M^{-1}cm^{-1}$): 520 (sh, 2510), 430 (8790), 330 (11760), 248 (30660).

Conversion of **2** to **1** with dioxygen: Pure dioxygen (4 mL) was introduced into a solution of **2** (0.045 g, 0.073 mmol) in MeCN (5 mL). The initial brown-red color changed immediately to purple-red. The reaction mixture was stirred for 2 h and then stored at −20 °C following the addition of dry Et_2O (7 mL). Deep-red crystals of **1** were formed within 4 h. The crystals were filtered and washed with dry Et_2O (0.04 g, yield: 86 %).

O-atom transfer reactions: To determine the rate of the O-atom transfer reaction for **1**, a solid portion of **1** (30 mg, 0.048 mmol) was added to a solution of PPh_3 (1.26 g, 4.80 mmol) in MeCN (10 mL). The reaction mixture was kept at 45 °C (or 65 °C) under 1 atm of dioxygen. Aliquots (100 μL) were taken out every 5 min and diluted to 10 mL with MeCN:H_2O (65:35). These samples were analyzed on a Spectra-Physics UV 2000 HPLC apparatus (Grace VYDAC reverse-phase C18 column, 5 μm particle size, 250 × 4.6 mm, 20 μL loop volume, flow rate: 1 mL min^{-1}) using isocratic elution with MeCN/H_2O (65:35).[15] Retention times for Ph_3PO and Ph_3P were 3.60 and 11.05 min, respectively. The areas under the peaks were determined by running authentic samples of known concentration under identical conditions. The rate was calculated from the slope of the plot of $-\ln[PPh_3]_t/[PPh_3]_o$ versus time (t). Only a trace amount of Ph_3PO was detected when a solution of PPh_3 in MeCN (without **1**) was heated at 65 °C for 1 h under 1 atm of dioxygen.

The O-atom transfer reactions were also studied by ^{31}P NMR spectroscopy (Varian Unity Plus spectrometer). Following incubation at 65 °C for various time intervals, the reaction mixtures were evaporated to dryness and extracted with ethyl acetate. The extracts were filtered to remove the catalyst (and its decomposition products) and the filtrates were again evaporated to dryness. The residues were dissolved in $CDCl_3$ (or CD_3CN) and their ^{31}P NMR spectra were obtained using H_3PO_4 as the internal standard in coaxial tubes (δ for PPh_3: −5 ppm; for Ph_3PO: 30 ppm in $CDCl_3$).

Received: June 5, 2003 [Z52070]

Keywords: heterogeneous catalysis · iron · N ligands · nitrogen oxides · phosphanes

[1] a) L. Cheng, D. R. Powell, M. A. Khan, G. B. Richter-Addo, *Chem. Commun.* **2000**, 2301 – 2302; b) O. Q. Munro, W. R. Scheidt, *Inorg. Chem.* **1998**, *37*, 2308 – 2316; c) M. Frangione, J. Port, M. Baldiwala, A. Judd, J. Galley, M. DeVega, K. Linna, L. Caron, E. Anderson, J. A. Goodwin, *Inorg. Chem.* **1997**, *36*, 1904 – 1911; d) C. E. Castro, S. K. O'Shea, *J. Org. Chem.* **1995**, *60*, 1922 – 1923; e) M. G. Finnegan, A. G. Lappin, W. R. Scheidt, *Inorg. Chem.* **1990**, *29*, 181 – 185.

[2] a) H. Adachi, H. Suzuki, Y. Miyazaki, Y. Limura, M. Hoshino, *Inorg. Chem.* **2002**, *41*, 2518 – 2524; b) J. Goodwin, R. Bailey, W. Pennington, R. Rasberry, T. Green, S. Shasho, M. Yongsavanh, V. Echevarria, J. Tiedeken, C. Brown, G. Fromm, S. Lyerly, N. Watson, A. Long, N. D. Nitto, *Inorg. Chem.* **2001**, *40*, 4217 – 4225.

[3] a) M. A. Andrews, T. C.-T. Chang, C.-W. F. Cheng, *Organometallics* **1985**, *4*, 268 – 274; b) M. A. Andrews, T. C.-T. Chang, C.-W. F. Cheng, T. J. Emge, K. P. Kelly, T. F. Koetzle, *J. Am. Chem. Soc.* **1984**, *106*, 5913 – 5920; c) D. T. Doughty, R. P. Stewart, Jr., G. Gordon, *J. Am. Chem. Soc.* **1981**, *103*, 3388 – 3395; d) R. D. Feltham, J. C. Kriege, *J. Am. Chem. Soc.* **1979**, *101*, 5064 – 5065; e) B. S. Tovrog, S. E. Diamond, F. Mares, *J. Am. Chem. Soc.* **1979**, *101*, 270 – 272.

[4] A. L. Feig, M. T. Bautista, S. J. Lippard, *Inorg. Chem.* **1996**, *35*, 6892 – 6898.

[5] W. T. Oosterhuis, G. Lang, *Phys. Rev.* **1969**, *178*, 439 – 456.

[6] Crystal data for $[(PaPy_3)Fe(NO_2)](ClO_4)\cdot 2\,CH_3CN$ (**1**·2 CH_3CN): Red blocks, 0.22 × 0.21 × 0.12 mm^3, monoclinic, space group $P2_1/n$, $a = 13.1985(4)$, $b = 14.1008(5)$, $c = 15.3473(5)$ Å, $\beta = 103.422(8)°$, $V = 2752(16)$ Å^3, $Z = 4$, $\rho_{calcd} = 1.520$ Mg m^{-3}, $2\theta_{max} = 63°$, $\mu(Mo_{K\alpha}) = 0.704$ mm^{-1}, $\lambda = 0.71073$ Å; the data were collected at 90(2) K on a Bruker SMART 1000 diffractometer; a total of 27326 reflections were measured, of which 8816 were independent ($R_{int} = 0.054$) and included in the refinement; min/max transmission = 0.8605/0.9203; solution by direct methods (SHELXL-97, Sheldrick, **1990**); refinement by full-matrix least-squares based on F^2 (SHELXL-97, Sheldrick, **1997**); 381 parameters, $R1 = 0.0693$, $wR2 = 0.1009$ for all data; $R1 = 0.0391$ computed for 8816 observed data ($I > 2\sigma(I)$).

[7] J. M. Rowland, M. Olmstead, P. K. Mascharak, *Inorg. Chem.* **2001**, *40*, 2810 – 2817.

[8] Crystal data for $[(PaPy_3)Fe(NO)](ClO_4)\cdot 2\,CH_3CN$ (**2**·2 CH_3CN): Brown-red plates, 0.30 × 0.16 × 0.08 mm^3; monoclinic, space

group $P2_1$, $a = 8.2530(4)$, $b = 13.9435(7)$, $c = 11.7823(6)$ Å, $\beta = 99.225(3)^{o}$, $V = 1338(12)$ Å^3, $Z = 2$, $\rho_{calcd} = 1.523$ Mg m^{-3}, $2\theta_{max} = 60°$, $\mu(Mo_{K\alpha}) = 0.719$ mm^{-1}, ω scans, $\lambda = 0.71073$ Å; the data were collected at 90(2) K on a Bruker SMART 1000 diffractometer; a total of 17556 reflections were measured, of which 7671 were independent ($R_{int} = 0.0305$) and included in the refinement; min/max transmission = 0.813/0.945; solution by direct methods; refinement by full-matrix least-squares based on F^2); 363 parameters, $R1 = 0.0376$, $wR2 = 0.0714$ for all data; $R1 = 0.0309$ computed for 6896 observed data ($I > 2\sigma(I)$).

[9] a) C. Hauser, T. Glaser, E. Bill, T. Weyhermuller, K. Wieghardt, *J. Am. Chem. Soc.* **2000**, *122*, 4352 – 4364; b) M. Ray, A. P. Golombek, M. P. Hendrich, G. P. A. Yap, L. M. Liable-Sands, A. L. Rheingold, A. S. Borovik, *Inorg. Chem.* **1999**, *38*, 3110 – 3115; c) D. Sellmann, N. Blum, F. W. Heinemann, B. A. Hess, *Chem. Eur. J.* **2001**, *7*, 1874 – 1880; d) D. Sellman, H. Kunstmann, M. Moll, F. Knoch, *Inorg. Chim. Acta* **1988**, *154*, 157 – 167; e) W. R. Scheidt, M. E. Frisse, *J. Am. Chem. Soc.* **1975**, *97*, 17 – 21; f) P. Berno, C. Floriani, A. Chiesi-Villa, C. Guastini, *J. Chem. Soc. Dalton Trans.* **1988**, 1409 – 1412.

[10] a) Crystal data for $[(PaPy_3)FeOFe(PaPy_3)](ClO_4)_2 \cdot 3\,EtOH$ (**3**·3 EtOH): Brown plate, $0.20 \times 0.06 \times 0.04$ mm^3; monoclinic, space group *C*2/*c*, $a = 17.649(3)$, $b = 13.383(2)$, $c = 22.371(4)$ Å, $\beta = 107.524(4)^{o}$, $V = 5038(15)$ Å^3, $Z = 4$, $\rho_{calcd} = 1.526$ Mg m^{-3}, $2\theta_{max} = 51°$, $\mu(Mo_{K\alpha}) = 0.758$ mm^{-1}, ω scans, $\lambda = 0.71073$ Å; the data were collected at 90(2) K on a Bruker SMART 1000 diffractometer; a total of 16306 reflections were measured, of which 4788 were independent ($R_{int} = 0.0772$) and included in the refinement; min/max transmission = 0.863/0.970; solution by direct methods; refinement by full-matrix least-squares based on F^2; 341 parameters, $R1 = 0.0940$, $wR2 = 0.1476$ for all data; $R1 = 0.0518$ computed for 3184 observed data ($I > 2\sigma(I)$); b) CCDC-211509 (**1**), -211510 (**2**), and -211511 (**3**) contains the supplementary crystallographic data for this paper. These data can be obtained free of charge via www.ccdc.cam.ac.uk/conts/retrieving.html (or from the Cambridge Crystallographic Data Centre, 12, Union Road, Cambridge CB21EZ, UK; fax: (+44) 1223-336-033; or deposit@ccdc.cam.ac.uk).

[11] A. K. Patra, M. M. Olmstead, P. K. Mascharak, *Inorg. Chem.* **2002**, *41*, 5403 – 5409.

[12] There is at least one example of such a nitrite-to-nitrosyl conversion in the case of a heme system. See reference [1a].

[13] Turnover numbers (TN) were obtained by dividing the total mass of Ph_3PO by the catalyst mass.

[14] The catalytic efficiency of the present system deserves attention since the only reported non-porphyrin system involving [Co(saloph)(py)(NO_2)] (saloph = *N*,*N*′-bisalicylidene-o-phenylenediamino) catalyzes the oxidation of PPh_3 with a TN of 8.7 after 16 h at 60 °C. See reference [3e].

[15] J. E. Haky, D. M. Baird, S. Falzone, *Anal. Lett.* **1989**, *22*, 2637 – 2651.

